J|A|C|S
ARTICLES
Published on Web 03/22/2007

Synthesis of Nitric Oxide-Releasing Silica Nanoparticles

Jae Ho Shin, Sara K. Metzger, and Mark H. Schoenfisch*

Contribution from the Department of Chemistry, the University of North Carolina at Chapel Hill, Chapel Hill, North Carolina 27599

Received October 17, 2006; E-mail: schoenfisch@unc.edu

Abstract: The synthesis and characterization of a new nitric oxide (NO)-releasing scaffold prepared from amine-functionalized silica nanoparticles are reported. Inorganic−organic hybrid silica was prepared via cocondensation of tetraethoxy- or tetramethoxysilane (TEOS or TMOS) and aminoalkoxysilane with appropriate amounts of ethanol (or methanol), water, and ammonia. The amine functional groups in the silica were converted to *N*-diazeniumdiolate NO donors via exposure to high pressures of NO (5 atm) under basic conditions. Control over both the structure and concentration of the silane precursors (i.e., tetraalkoxy- and aminoalkoxysilanes) and specific synthetic conditions allowed for the preparation of NO donor silica particles of widely varying sizes (d = 20−500 nm), NO payloads (50−1780 nmol·mg^{-1}), maximum amounts of NO released (10−5500 ppb·mg^{-1}), half-lives (0.1−12 h), and NO release durations (up to 30 h). The silica nanoparticles were characterized by solid-state ^{29}Si nuclear magnetic resonance (NMR), atomic force microscopy (AFM), elemental analysis, and gas adsorption−desorption isotherms. The advantages of silica-derived NO storage/delivery systems over previously reported macromolecular NO donors include the ability to (1) store large quantities of NO, (2) modulate NO release kinetics, and (3) readily tune particle size based on the composition of the particle. In addition, a one-pot strategy for preparing the NO donor silica allows for straightforward, high-throughput synthesis and purification.

Introduction

Nitric oxide (NO) is a diatomic free radical endogenously synthesized in the human body when L-arginine is converted to L-citrulline by a class of enzymes known as nitric oxide synthase (NOS).[1,2] Since the first reports describing NO's action as an endothelium-derived relaxation factor (EDRF) in the mid-1980s, much research has been devoted to elucidating the pathways of NO generation and action in vivo.[3] To date, researchers have discovered that NO regulates a range of biological processes in the cardiovascular, gastrointestinal, genitourinary, respiratory, and central and peripheral nervous systems.[2,4] Furthermore, the discoveries of NO as a vasodilator,[5] antibacterial agent,[6,7] and tumoricidal factor[8−10] have made NO a promising pharmaceutical agent. To further comprehend the complex and wide-ranging roles of NO and facilitate its therapeutic use, a number of synthetic compounds that chemically store and release NO in a controlled fashion have been developed.

Several classes of NO donors exist including nitrosothiols, nitrosamines, diazeniumdiolates, NO−metal complexes, and organic nitrites and nitrates.[11,12] Of these, 1-amino-substituted diazen-1-ium-1,2-diolates (or simply *N*-diazeniumdiolates) are particularly attractive due to their ability to generate NO spontaneously under biological conditions.[13,14] Since the first report on the synthesis of *N*-diazeniumdiolates via the reaction of amines with NO at elevated pressure in the 1960s,[15,16] several *N*-diazeniumdiolate compounds have been synthesized using a range of nucleophilic residues that encompass primary and secondary amines, polyamines, and secondary amino acids.[13] While stable under ambient conditions, *N*-diazeniumdiolates decompose spontaneously in aqueous media to generate NO at rates dependent upon pH, temperature, and the structure of the amine moiety.[13] For example, *N*-diazeniumdiolate-modified proline (PROLI/NO), 2-(dimethylamino)ethylputreanine (DMAEP/NO), *N*,*N*′-dimethylhexanediamine (DMHD/NO), and diethylenetriamine (DETA/NO) have been developed as effective small molecule NO donors with diverse NO release half-lives ranging from 2 s to 20 h at pH 7.4 and 37 °C.[13,17]

(1) Butler, A. R.; Nicholson, R. *Life, Death and Nitric Oxide*; Royal Society of Chemistry: Cambridge, 2003.
(2) Ignarro, L. J. *Nitric Oxide: Biology and Pathobiology*; Academic Press: San Diego, CA, 2000.
(3) Ignarro, L. J.; Bugga, G. M.; Wood, K. S.; Byrns, R. E.; Chaudhuri, G. *Proc. Natl. Acad. Sci. U.S.A* **1987**, *84*, 9265−9269.
(4) Moncada, S.; Higgs, A. *N. Engl. J. Med.* **1993**, *30*, 2002−2011.
(5) Radomski, M. W.; Palmer, R. M. J.; Moncada, S. *Br. J. Pharmacol.* **1987**, *92*, 639−646.
(6) Albina, J. E.; Reichner, J. S. *Cancer Metastasis Rev.* **1998**, *17*, 19−53.
(7) Nablo, B. J.; Chen, T.-Y.; Schoenfisch, M. H. *J. Am. Chem. Soc.* **2001**, *123*, 9712−9713.
(8) Cobbs, C. S.; Brenman, J. E.; Aldape, K. D.; Bredt, D. S.; Israel, M. A. *Cancer Res.* **1995**, *55*, 727−730.
(9) Jenkins, D. C.; Charles, I. G.; Thomsen, L. L.; Moss, D. W.; Holmes, L. S.; Baylis, S. A.; Rhodes, P.; Westmore, K.; Emson, P. C.; Moncada, S. *Proc. Natl. Acad. Sci. U.S.A.* **1995**, *92*, 4392−4396.
(10) Thomsen, L. L.; Miles, D. W.; Happerfield, L.; Bobrow, L. G.; Knowles, R. G.; Moncada, S. *Br. J. Cancer* **1995**, *72*, 41−44.
(11) Wang, P. G.; Cai, T. B.; Taniguchi, N. *Nitric Oxide Donors: For Pharmaceutical and Biological Applications*; Wiley-VCH: Weinheim, Germany, 2005.
(12) Wang, P. G.; Xian, M.; Tang, X.; Wu, X.; Wen, Z.; Cai, T.; Janczuk, A. J. *Chem. Rev.* **2002**, *102*, 1091−1134.
(13) Hrabie, J. A.; Keefer, L. K. *Chem. Rev.* **2002**, *102*, 1135−1154.
(14) Napoli, C.; Ignarro, L. J. *Annu. Rev. Pharmacol. Toxicol.* **2003**, *43*, 97−123.
(15) Drago, R. S.; Karstetter, B. R. *J. Am. Chem. Soc.* **1961**, *83*, 1819−1822.
(16) Drago, R. S.; Paulik, F. E. *J. Am. Chem. Soc.* **1960**, *82*, 96−98.

10.1021/ja0674338 CCC: $37.00

Considerable effort has been devoted to developing NO storage/delivery systems whereby such NO donors are attached to macromolecular frameworks.[18−22] Such scaffolds possess large quantities of NO with readily modifiable NO release kinetics. For example, Pulfer et al. reported the synthesis of *N*-diazeniumdiolate-modified polyethyleneimine microspheres ($d = 10-50$ μm) that were embedded into vascular grafts to prevent thrombosis and restenosis.[20] Likewise, Hrabie et al. synthesized water-soluble NO donor−protein conjugates via covalent attachment of methoxymethyl-protected *N*-diazeniumdiolated piperazine (MOM-PIPERAZI/NO) ligands to the lysine residues of both bovine and human serum albumin.[18] Jeh et al. demonstrated the delivery of NO to the alveolar region of the lungs via inhalable, biodegradable microparticles ($d = 10-35$ μm) prepared using poly(lactic-*co*-glycolic acid) or polyethylene oxide-*co*-lactic acid copolymer that encapsulated small molecule NO donors (e.g., PROLI/NO).[19] More recently, our laboratory has focused on the synthesis and characterization of NO-releasing monolayer-protected gold clusters[21] and dendrimer conjugates.[22] Despite their small size, unprecedented NO release properties, and potential for targeting the delivery of NO, the complex synthesis and potential toxicity of the gold cluster and dendrimer constructs remain notable concerns.

Inorganic−organic hybrid silica nanoparticles, functionalized ceramic materials prepared from silicon dioxide, have been employed as carrier systems for the controlled delivery of drugs, genes, and proteins.[23−27] The drug delivery potential of silica has received much attention because of its physical and chemical versatility (e.g., ability to tune the mesoporous structure and control specific surface properties) and nontoxic nature.[28−31] The synthesis of inorganic−organic hybrid silica modified with reactive organic groups (e.g., amines, carboxylates, thiols, olefins, halides, and epoxides) capable of further functionalization with deliverable molecules has been reported.[30,31] Indeed, silane-coupling agents with the aforementioned functional moieties are available for surface grafting (via free silanol groups) of drugs and other therapeutics.[32] Zhang et al. previously reported the synthesis of NO-releasing fumed silica (amorphous particles of $d = 0.2-0.3$ μm) via grafting amine-functionalized silylation reagents onto the silica surface and then converting the amines to *N*-diazeniumdiolates.[33] Despite the unique advantages of combining the *N*-diazeniumdiolate chemistry with the versatility of micro- and nanocomposite materials, the usefulness of such scaffolds as therapeutic NO delivery systems remains hindered due to limited control over size and NO storage.

Herein, we report a new synthetic approach to preparing NO-releasing silica nanoparticles via a one-pot[31,34,35] sol−gel process (Scheme 1) followed by exposure to 5 atm of NO under basic conditions. Amine-functionalized hybrid silica composites were prepared via cocondensation of tetraethoxy- or tetramethoxysilane (TEOS or TMOS) and aminoalkoxysilane with appropriate amounts of ethanol (or methanol), water, and ammonia. The amine functional groups within the silica particles were subsequently converted to *N*-diazeniumdiolate NO donors via exposure to high pressures of NO (5 atm) in the presence of sodium methoxide (NaOMe) base.[13] The advantage of a one-pot approach for preparing the silica is that the *N*-diazeniumdiolate NO donor precursors are distributed uniformly throughout the particle as opposed to only at the surface (as is the case for amine-modified silica[33] or gold particles[21] formed via surface-grafting methods). The selection of the silane precursors (e.g., type and concentration) and specific reaction/processing conditions (e.g., solvent, catalyst, pH, and temperature) allows for tremendous chemical flexibility in creating nanoparticles of diverse size[31,36] and NO release properties (e.g., NO payload and delivery kinetics).

Experimental Section

Reagents and Materials. Tetraethoxysilane (TEOS), tetramethylsilane (TMS), and sodium methoxide (NaOMe) were purchased from Fluka (Buchs, Switzerland). (Aminoethylamino-methyl)phenethyltrimethoxysilane (AEMP3), *N*-(6-aminohexyl)aminopropyltrimethoxysilane (AHAP3), and *N*-(2-aminoethyl)-3-aminopropyltrimethoxysilane (AEAP3) were purchased from Gelest (Tullytown, PA). Tetramethoxysilane (TMOS) and *N*,*N*-dimethylformamide (DMF) were purchased from Sigma (St. Louis, MO). Methanol (MeOH), ethanol (EtOH), tetrahydrofuran (THF), toluene, and ammonia solution (NH_4OH, 30 wt % in water) were purchased from Fisher Scientific (Fair Lawn, NJ). One-component room-temperature vulcanizing (RTV)-type silicone rubber (SR, 3140 RTV) was purchased from Dow Corning (Midland, MI). Tecophilic polyurethane (PU, HP-93A-100) was a gift from Noveon (Cleveland, OH). Nitric oxide (NO, 99.5%), argon (Ar), and nitrogen (N_2) gases were obtained from AGA Gas (Maumee, OH) or National Welders Supply (Raleigh, NC). Other solvents and chemicals were analytical−reagent grade and used as received. A Millipore Milli-Q UV Gradient A10 System (Bedford, MA) was used to purify distilled water to a final resistivity of 18.2 MΩ•cm and a total organic content of ≤6 ppb.

Synthesis of Nitric Oxide-Releasing Silica Nanoparticles. Amine-functionalized silica composite particles were synthesized via a cocondensation process (Scheme 1).[31,34,35] First, the silane solutions were prepared by mixing 2.78 mmol of TEOS or TMOS with different concentrations of AEAP3, AHAP3, or AEMP3 (0−18.6 mmol corresponding to 0−87 mol %, balance TEOS or TMOS) for 5 min. The silane solution was then combined with 22 mL of EtOH or MeOH and 6 mL of ammonia (30 wt % in water) and vigorously stirred for 30 min under ambient conditions. The white precipitate was collected by

(17) Keefer, L. K. *Annu. Rev. Pharmacol. Toxicol.* **2003**, *43*, 585−607.
(18) Hrabie, J. A.; Saavedra, J. E.; Roller, P. P.; Southan, G. J.; Keefer, L. K. *Bioconjugate Chem.* **1999**, *10*, 838−842.
(19) Jeh, H. S.; Lu, S.; George, S. C. *J. Microencapsulation* **2004**, *21*, 3−13.
(20) Pulfer, S. K.; Ott, D.; Smith, D. J. *J. Biomed. Mater. Res.* **1997**, *37*, 182−189.
(21) Rothrock, A. R.; Donkers, R. L.; Schoenfisch, M. H. *J. Am. Chem. Soc.* **2005**, *127*, 9362−9363.
(22) Stasko, N. A.; Schoenfisch, M. H. *J. Am. Chem. Soc.* **2006**, *128*, 8265−8271.
(23) Lai, C.-Y.; Trewyn, B. G.; Jeftinija, D. M.; Jeftinija, K.; Xu, S.; Jeftinija, S.; Lin, V. S.-Y. *J. Am. Chem. Soc.* **2003**, *125*, 4451−4459.
(24) Munoz, B.; Ramila, A.; Perez-Pariente, J.; Diaz, I.; Vallet-Regi, M. *Chem. Mater.* **2003**, *15*, 500−503.
(25) Roy, I.; Ohulchanskyy, T. Y.; Bharali, D. J.; Pudavar, H. E.; Mistretta, R. A.; Kaur, N.; Prasad, P. N. *Proc. Natl. Acad. Sci. U.S.A.* **2005**, *102*, 279−284.
(26) Trewyn, B. G.; Whitman, C. M.; Lin, V. S.-Y. *Nano Lett.* **2004**, *4*, 2139−2143.
(27) Yoshitake, H. *New J. Chem.* **2005**, *29*, 1107−1117.
(28) Kim, J. S.; Yoon, T. J.; Yu, K. N.; Kim, B. G.; Park, S. J.; Kim, H. W.; Lee, K. H.; Park, S. B.; Lee, J. K.; Cho, M. H. *Toxicol. Sci.* **2006**, *89*, 338−347.
(29) Kneuer, C.; Sameti, M.; Haltner, E. G.; Schiestel, T.; Schirra, H.; Schmidt, H.; Lehr, C. M. *Int. J. Pharm.* **2000**, *196*, 257−261.
(30) Sayari, A.; Hamoudi, S. *Chem. Mater.* **2001**, *13*, 3151−3168.
(31) Stein, A.; Melde, B. J.; Schroden, R. C. *Adv. Mater.* **2000**, *12*, 1403−1419.
(32) Anwander, R.; Palm, C.; Stelzer, J.; Groeger, O.; Engelhardt, G. *Stud. Surf. Sci. Catal.* **1998**, *117*, 135−142.
(33) Zhang, H.; Annich, G. M.; Miskulin, J.; Stankiewicz, K.; Osterholzer, K.; Merz, S. I.; Bartlett, R. H.; Meyerhoff, M. E. *J. Am. Chem. Soc.* **2003**, *125*, 5015−5024.
(34) Hatton, B.; Landskron, K.; Whitnall, W.; Perovic, D.; Ozin, G. *Acc. Chem. Res.* **2005**, *38*, 305−312.
(35) Lin, H.-P.; Mou, C.-Y. *Acc. Chem. Res.* **2002**, *35*, 927−935.
(36) Lim, M. H.; Stein, A. *Chem. Mater.* **1999**, *11*, 3285−3295.

Scheme 1. Synthesis of *N*-Diazeniumdiolate-Modified Silica Nanoparticles Using Tetramethoxysilane (TMOS) and *N*-(6-Aminohexyl)aminopropyltrimethoxysilane (AHAP3) as Example Tetraalkoxy- and Aminoalkoxysilane Precursors

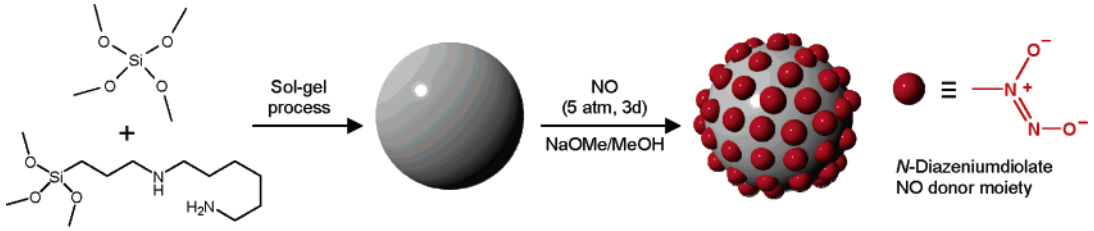

centrifugation (5000 rpm, 5 min), washed copiously with EtOH, and dried under vacuum overnight.

The resulting amine-functionalized silica was resuspended in 18 mL of DMF and 2 mL of MeOH in the presence of NaOMe (0.32−18.6 mmol; adding an equimolar amount of NaOMe corresponding to the secondary amine content of silica composites)[13,33] and placed in 10 mL vials equipped with a stir bar. The vials were placed in a Parr bottle (200 mL), connected to an in-house NO reactor, and flushed with Ar for 10 min six times to remove oxygen in the suspension. The reaction bottle was then charged with NO to 5 atm and sealed for 3 d while stirring. The NO gas was purified over KOH pellets for 2 h to remove trace NO degradation products. Prior to removing the silica particles, unreacted NO was purged from the chamber with Ar. The *N*-diazeniumdiolate-modified silica particles were recollected by centrifugation at 5000 rpm for 5 min, washed copiously with EtOH, dried under ambient conditions for 1 h, and stored in a sealed container at −20 °C until used.

Characterization of Functionalized Silica. Prior to analysis via atomic force microscopy (AFM), the silica particles were suspended in toluene, deposited on a freshly cleaved mica surface (SPI; West Chester, PA), and dried under ambient conditions for 3 h. Contact mode AFM images were obtained in air using a Molecular Force Probe 3D atomic force microscope (Asylum Research; Santa Barbara, CA) controlled with MFP-3D software running under Igor Pro (Wavemetrics; Lake Oswego, OR). Triangular silicon nitride cantilevers with a nominal spring constant of 0.12 $N \cdot m^{-1}$ and resonance frequency of 20 kHz (Veeco; Santa Barbara, CA) were used to acquire height/topography images at a scan rate of 0.5 Hz.

Solid-state cross-polarization/magic angle spinning (CP/MAS) ^{29}Si nuclear magnetic resonance (NMR) spectra[37,38] were obtained at 293 K on a Bruker 360 MHz DMX spectrometer (Billerica, MA) equipped with wide-bore magnets (triple-axis pulsed field gradient double-resonance probes). Silica composite particles were packed into 4 mm rotors (double-resonance frequency of 71.548 MHz) and spun at a speed of 8.0 kHz. The chemical shifts were determined in ppm relative to a TMS external standard.

Nitric oxide release profiles of the *N*-diazeniumdiolate-modified silica nanoparticles were measured in deoxygenated phosphate-buffered saline (PBS, 0.01 M; 37 °C) at pH values of 3.3, 4.3, 5.3, 6.0, 7.4, and 9.5 using a Sievers NOA 280i chemiluminescence nitric oxide analyzer (Boulder, CO).[22,39] Nitric oxide released from the silica was transported to the analyzer by a stream of N_2 (70 $mL \cdot min^{-1}$) passed through the reaction cell. The instrument was calibrated with air passed through a zero filter (0 ppm NO) and 24.1 ppm of NO standard gas (balance N_2, purchased from AGA Gas).

The surface area and pore volume of the silica were determined via nitrogen adsorption/desorption isotherms[38] collected with a Beckman Coulter SA3100 surface area and pore size analyzer (Fullerton, CA). The surface area and pore volume were calculated using the Brunauer−Emmett−Teller (BET) and Barrett−Joyner−Halenda (BJH) methods. Prior to the measurements, all silica samples were degassed at 200 °C for 3 h.

Elemental (CHN) analyses were performed by Midwest Microlab, LLC (Indianapolis, IN) to determine the concentration of amines incorporated in the functionalized silica nanoparticles.

Preparation and Characterization of NO-Releasing Silica/Polymer Hybrid Films. Hybrid silica/polymer films were formed on glass slides (Area = 2.0 cm^2) by casting 50 μL of PU or SR cocktail prepared by dissolving 50 mg of PU or 200 mg of SR and 30 mg of NO donor silica nanoparticles (77 mol % AHAP3, balance TMOS) in 1500 μL of THF. The NO release from the silica-doped polymers was evaluated in deoxygenated PBS at 37 °C and pH 7.4 as described above. Surface wettability of the films was characterized by measuring static water contact angles with a KSV Instruments Cam 200 optical contact angle meter (Helsinki, Finland).

Results and Discussion

Synthesis and Characterization of Functionalized Silica Nanoparticles. To synthesize organically-modified hybrid silica via co-condensation of two silicon alkoxide precursors, tetramethoxy- and tetraethoxysilanes (TMOS and TEOS), were used as backbone silanes.[40] The choice of the tetraalkoxysilane is crucial for the formation of silica composites with homogeneous distributions of active functionalities.[41−43] For example, differences in the hydrolysis and condensation rates of tetraalkoxy- and organoalkoxysilanes often result in disordered, inhomogeneous silica.[36,41,42,44] As such, matching the hydrolysis and condensation rates of bi- and multicomponent silane systems plays an important role in synthesizing well-ordered, mesoporous materials.[36,41,42,44] In general, the following factors can be used to predict hydrolysis and condensation propensities of the silanes: (1) a methoxy ligand is more readily hydrolyzed than an ethoxy one; (2) the hydrolysis of organoalkoxysilanes is slower than fully hydrolyzable tetraalkoxysilane with the same alkoxy identity; (3) the long alkyl chain, steric hindrance, and hydrophobic nature of the organic group often impede the overall hydrolytic polycondensation reactions.[36,41,42,44] With these factors in mind, TEOS was selected as the initial silicon alkoxide backbone for study because of its similar hydrolysis rate to that of the aminoalkoxysilanes (i.e., AHAP3, AEAP3, and AEMP3) used in this study.

Control over both the structure and concentration of the aminoalkoxysilane precursors and specific synthetic conditions

(37) Albert, K.; Bayer, E. *J. Chromatogr.* **1991**, *544*, 345−370.
(38) Huh, S.; Wiench, J. W.; Yoo, J.-C.; Pruski, M.; Lin, V. S.-Y. *Chem. Mater.* **2003**, *15*, 4247−4256.
(39) Beckman, J. S.; Conger, K. A. *Methods Companion Methods Enzymol.* **1995**, *7*, 35−39.
(40) Brinker, C. J.; Scherer, G. *Sol−Gel Science: The Physics and Chemistry of Sol−Gel Processing*; Academic Press: Boston, MA, 1989.
(41) Pagliaro, M.; Ciriminna, R.; Man, M. W. C.; Campestrini, S. *J. Phys. Chem. B* **2006**, *110*, 1976−1988.
(42) Wight, A. P.; Davis, M. E. *Chem. Rev.* **2002**, *102*, 3589−3614.
(43) Melero, J. A.; van Grieken, R.; Morales, G. *Chem. Rev.* **2006**, *106*, 3790−3812.
(44) Liu, J.; Yang, Q.; Kapoor, M. P.; Setoyama, N.; Inagaki, S.; Yang, J.; Zhang, L. *J. Phys. Chem. B* **2005**, *109*, 12250−12256.

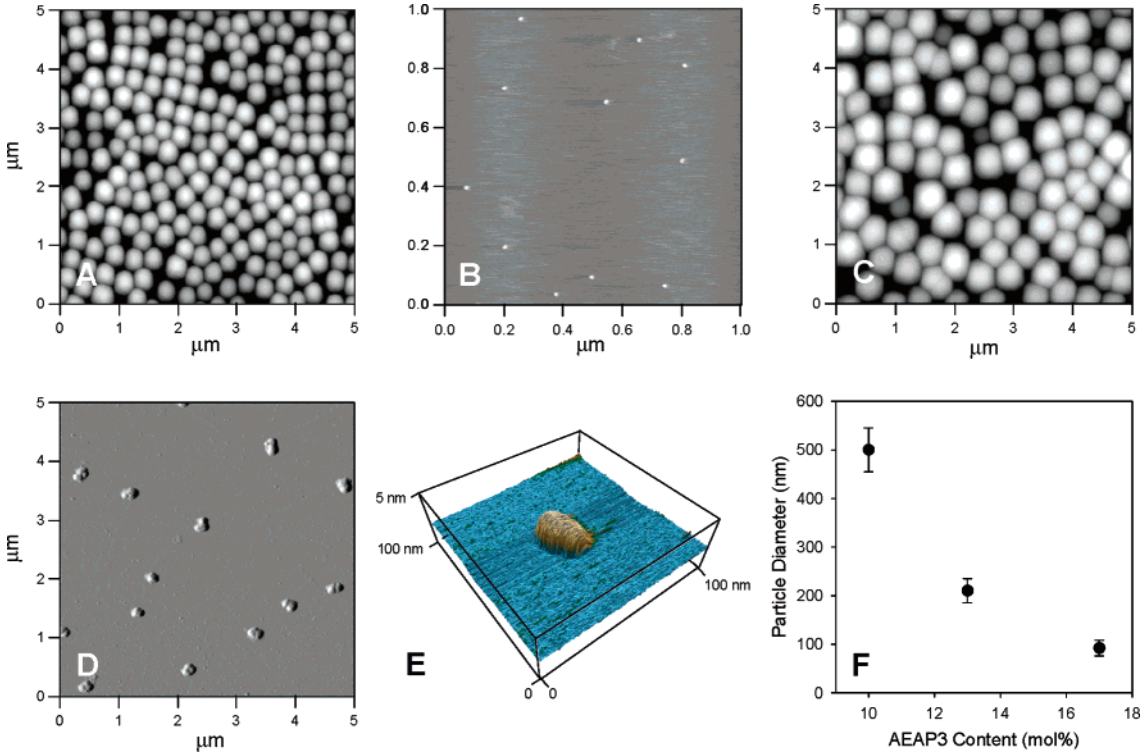

Figure 1. Contact mode AFM images of (A) control silica (TEOS only), (B) silica with 10 mol % of AHAP3 (balance TEOS), and (C) 10 mol % and (D) 17 mol % AEAP3 silica particles on a mica surface. (E) Enlargement of a single particle from (B). (F) Relationship between the AEAP3 content (balance TEOS) in the silica composite and particle size.

allowed for the preparation of NO donor silica nanoparticles of widely varying size and NO release properties. As shown in Figure 1, the size of the silica nanoparticles was tunable by varying the type and concentration of aminoalkoxysilane used. The diameter of control (TEOS only) silica particles was 250 ± 20 nm. Adding 10 mol % AHAP3 to the TEOS solution decreased the diameter of the particles to 20 ± 2 nm. In contrast, silica particles prepared from 10 mol % AEAP3 (balance TEOS) were roughly twice as large (d = 500 ± 45 nm) as TEOS controls. As the mol % of AEAP3 was increased from 10 to 17 mol %, the diameter of the particle decreased to 92 ± 16 nm, revealing a pseudolinear relationship between particle size and aminoalkoxysilane concentration (Figure 1F). Particle size was not altered upon conversion of the amines to *N*-diazeniumdiolates, indicating that the structural integrity of the silica particles is not compromised by the conditions necessary to form the NO donor (data not shown).

Solid-state ^{29}Si NMR was used to (1) confirm the incorporation of aminoalkyl functionalities within the silica network (Figure 2) and (2) determine the surface coverage of such ligands (Supporting Information).[38] Cross-polarization and magic angle spinning (CP/MAS) techniques were employed to increase the signal resolution and sensitivity. The spectra for control and amine-functionalized silica particles prepared from 0 and 10−17 mol % AEAP3 (balance TEOS) are shown in Figure 2. For TEOS control silica, three distinct peaks in the ^{29}Si NMR spectrum were observed at −90, −101, and −109 ppm, respectively, representative of Q^2 (geminal silanol; $-O_2Si(OH)_2$), Q^3 (single silanol; $-O_3Si(OH)$), and Q^4 (siloxane; $-O_4Si$) silicons.[37,38] For the aminoalkoxysilane-modified silica particles, five peaks were observed in the spectra, indicating two additional silicon chemical environments (graphs b−d in Figure 2A). Indeed, the peaks at chemical shifts of approximately −52 and −65 ppm are representative of silicon connected to T^2 ($-O_2Si(OH)R$) and T^3 ($-O_3SiR$) structures, respectively (where R is an aminoethylaminopropyl group).[37,38] The presence of T^n bands suggests the existence of covalent linkages between aminoalkyl groups and the silica backbone. The Q^2, Q^3, and Q^4 resonance lines also appeared at the expected positions. As the AEAP3 content was increased from 10 to 17 mol %, the surface coverage of aminoalkyl ligands [SC = $(T^2 + T^3)/(T^2 + T^3 + Q^2 + Q^3)$][38,45] increased from 21% to 37% (Figure 2C), respectively. The ligand immobilization efficiency (e_{immo}), defined as the ratio of % SC and AEAP3 content (mol %) incorporated in the starting sol, was between 2.1 and 2.6, indicating effective immobilization of aminoalkyl groups. Of note, the integration and quantitative analysis of these structures are complicated because the intensity of each peak depends on the efficiency of cross polarization and the proton relaxation time.[46]

The surface area and pore volume of the silica nanoparticles were evaluated via nitrogen adsorption−desorption isotherms.[38] As expected, the amine-functionalized silica proved to be nonporous with surface areas (S_{BET}) of 10−20 $m^2 \cdot g^{-1}$ and pore volumes (V_p) of 0.02−0.06 $mL \cdot g^{-1}$ (at p/p_0 = 0.98). Indeed, previous reports of organically modified hybrid silica synthesized by the cocondensation method indicated highly dense, nonporous, and amorphous structures.[30,31]

Nitric Oxide Release Characteristics. Nitric oxide release was evaluated as a function of tetraalkoxy- and aminoalkoxysilane structure and concentration. The NO release profiles of two representative silica nanoparticles (10 mol % AHAP3 and 17 mol % AEAP3, balance TEOS) are shown in Figure 3. These

(45) Radu, D. R.; Lai, C.-Y.; Wiench, J. W.; Pruski, M.; Lin, V. S.-Y. *J. Am. Chem. Soc.* **2004**, *126*, 1640−1641.
(46) Bruch, M. D.; Fatunmbi, H. O. *J. Chromatogr., A* **2003**, *1021*, 61−70.

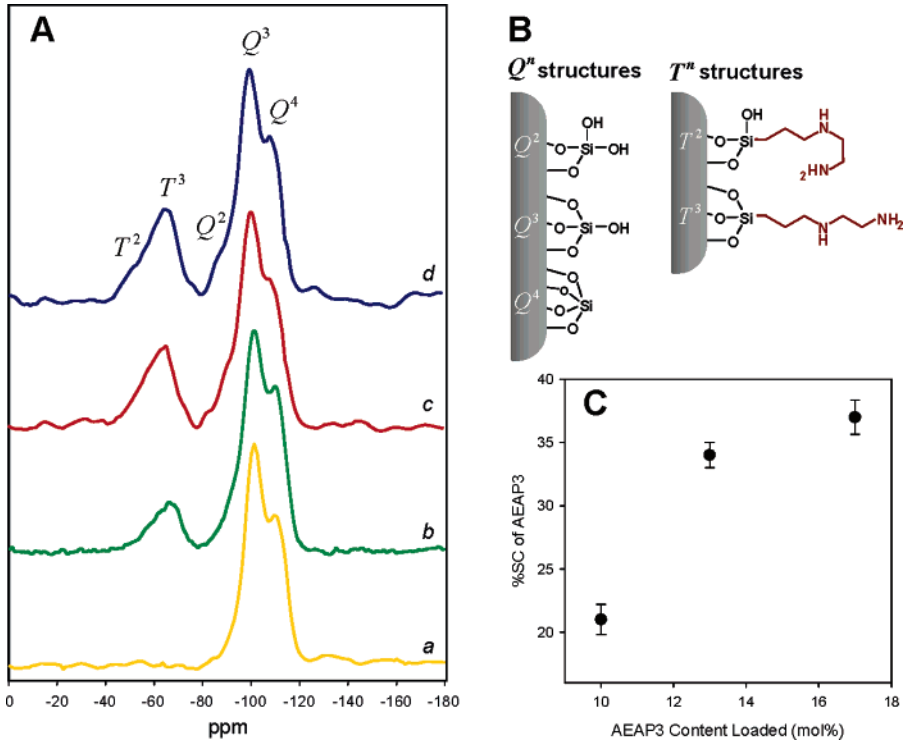

Figure 2. (A) Solid-state ^{29}Si CP/MAS NMR spectra of functionalized silica materials with various amounts of AEAP3: (a) 0 (control), (b) 10, (c) 13, and (d) 17 mol % (balance TEOS). (B) Schematic illustration of silicon chemical environments at the surface of AEAP3-modified silica composites. (C) Plot of percent surface coverage (% SC) of functional ligands vs AEAP3 content loaded during the synthesis.

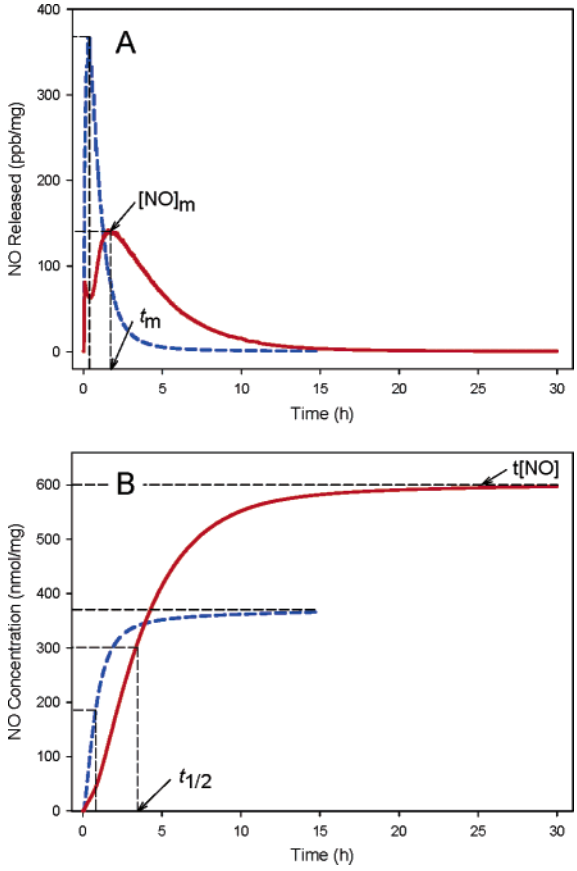

Figure 3. (A) NO release profiles and (B) total NO release of 10 mol % AHAP3 (dashed blue curve) and 17 mol % of AEAP3 (solid red curve) silica nanoparticles (balance TEOS).

representative compositions illustrate the drastic effects of amine derivatization on several NO release properties including the total amount of NO (t[NO]), half-life of NO release ($t_{1/2}$), maximum concentration of NO release ($[NO]_m$), and time necessary to reach $[NO]_m$ (t_m). Both the NO payload and release rates were significantly affected by the concentration and chemical identity of the amine ligands (e.g., AEAP3, AHAP3, and AEMP3) used to prepare the silica nanoparticles (Table 1). At a fixed aminoalkoxysilane concentration of 10 mol % (balance TEOS), the trend in t[NO] was AHAP3 > AEAP3 > AEMP3 (380, 145, and 53 nmol·mg^{-1}, respectively). For AEAP3 and AEMP3 silica, increasing the concentration of aminoalkoxysilanes from 10 to 20 mol % led to notable increases in both t[NO] and $[NO]_m$. For the AEAP3 system, both the $t_{1/2}$ and t_m decreased with increasing aminoalkoxysilane concentration (from 12 to 3.4 h and 8.0 to 2.1 h for 10 to 17 mol % AEAP3 silica, respectively).

The decrease in NO release kinetics corresponded directly with nanoparticle size and predicted water uptake. A shorter water diffusion distance to interior NO donor ligands would be expected for smaller diameter particles, resulting in more rapid *N*-diazeniumdiolate breakdown and NO release. For AEMP3 silica nanoparticles, the $t_{1/2}$ and t_m were constant regardless of the aminoalkoxysilane concentration. Such fixed NO release kinetics for AEMP3 was expected due to the similar size of the particles (~30 to 50 nm) over the range of aminoalkoxysilane concentrations studied (i.e., 10−20 mol %, balance TEOS). As shown in Table 2, the amine to *N*-diazeniumdiolate conversion efficiencies for the TEOS-derived silica nanoparticles ranged from ~6% to 19%, depending on the size and composition of the nanoparticle. Larger silica nanoparticles were characterized by lower conversion efficiencies than smaller sized particles (e.g., 6% vs 15% for 10 and 17 mol % AEAP3 silica, respectively). Similar to other *N*-diazeniumdiolate NO donor scaffolds, the mechanism of NO release was proton initiated as

Table 1. NO Release Properties of *N*-Diazeniumdiolate-Modified Silica Nanoparticles with Different Tetraalkoxy- and Aminoalkoxysilane Precursors[a,b]

	aminoalkoxysilane						
tetraalkoxysilane[c]	type[d]	mol %[e]	particle size (nm)[f]	t[NO] (nmol·mg^{-1})	$t_{1/2}$ (h)	[NO]$_m$ (ppb·mg^{-1})	t_m (h)
TEOS	AEMP3	10	50 ± 5	53 ± 3	6.0 ± 0.2	10 ± 2	0.12 ± 0.01
		13	43 ± 4	81 ± 3	6.5 ± 0.3	22 ± 2	0.10 ± 0.01
		17	40 ± 5	118 ± 5	5.7 ± 0.5	32 ± 2	0.11 ± 0.02
		20	30 ± 4	170 ± 10	5.4 ± 0.3	40 ± 3	0.11 ± 0.01
	AEAP3	10	500 ± 45	145 ± 10	12 ± 4	14 ± 3	8 ± 1
		13	210 ± 25	392 ± 15	6 ± 1.5	92 ± 5	4 ± 1
		17	92 ± 16	600 ± 25	3.4 ± 0.4	140 ± 10	2.1 ± 0.3
	AHAP3	10	20 ± 2	380 ± 20	0.9 ± 0.1	370 ± 10	0.35 ± 0.05
TMOS	AEAP3	10	270 ± 25	46 ± 4	1.9 ± 0.3	40 ± 7	0.18 ± 0.04
		30	130 ± 10	156 ± 10	1.7 ± 0.1	146 ± 20	0.08 ± 0.01
		50	98 ± 8	308 ± 35	1.9 ± 0.4	308 ± 100	0.25 ± 0.04
		70	74 ± 8	414 ± 20	1.6 ± 0.1	1100 ± 240	0.14 ± 0.01
		87	58 ± 10	330 ± 10	0.1 ± 0.02	5500 ± 300	0.06 ± 0.01
	AHAP3	10	64 ± 4	101 ± 5	0.2 ± 0.04	560 ± 40	0.07 ± 0.02
		30	55 ± 5	230 ± 4	0.3 ± 0.09	730 ± 290	0.10 ± 0.03
		50	51 ± 6	440 ± 30	0.7 ± 0.2	510 ± 30	0.11 ± 0.04
		60	58 ± 5	680 ± 40	0.5 ± 0.01	1900 ± 190	0.07 ± 0.01
		70	48 ± 7	1700 ± 20	0.9 ± 0.01	2660 ± 190	0.12 ± 0.07
		77	65 ± 5	1780 ± 50	0.9 ± 0.2	2810 ± 210	0.11 ± 0.3
	2N[2][g]		200−300	580	2.4		
	2N[6][g]		200−300	560 ± 60	0.7		

[a] n is at least 3. [b] Values were measured in deoxygenated phosphate-buffered saline (PBS) at pH 7.4 and 37 °C. [c] TEOS, tetraethoxysilane; TMOS, tetramethoxysilane. [d] AEMP3, (aminoethylaminomethyl)phenethyltrimethoxysilane; AEAP3, *N*-(2-aminoethyl)-3-aminopropyltrimethoxysilane; AHAP3, *N*-(6-aminohexyl)aminopropyltrimethoxysilane. [e] Balance TEOS or TMOS. [f] Diameter. [g] Reference 33. Amine-modified silica particles were prepared via the surface-grafting method.

Table 2. Nitrogen Content (% N), Amine Concentration (C_{amine}), *N*-Diazeniumdiolate Concentration (C_{diaz}), and Amine to *N*-Diazeniumdiolate Conversion Efficiency (% Conv) of Various Silica Nanoparticles Prepared with Different Tetraalkoxy- and Aminoalkoxysilane Precursors

	aminoalkoxysilane					
tetraalkoxysilane[a]	type[b]	mol %[c]	% N[d]	C_{amine} (μmol·mg^{-1})[e]	C_{diaz} (μmol·mg^{-1})[f]	% conv
TEOS	AEAP3	10	3.39	1.21	0.07	5.8
		13	3.90	1.39	0.20	14.4
		17	5.45	1.95	0.30	15.4
	AHAP3	10	2.74	0.98	0.19	19.4
TMOS	AEAP3	30	1.94	0.69	0.08	11.6
		50	2.91	1.04	0.15	14.4
		70	3.69	1.32	0.21	15.9
		87	3.22	1.15	0.17	14.8
	AHAP3	10	1.45	0.52	0.05	9.6
		30	2.84	1.01	0.11	10.9
		50	3.12	1.11	0.22	19.8
		60	4.19	1.50	0.34	22.7
		70	4.74	1.69	0.85	50.3
		77	4.81	1.72	0.89	51.7
	2N[2][g]			1.23	0.29	24
	2N[6][g]			0.86	0.28	33

[a] TEOS, tetraethoxysilane; TMOS, tetramethoxysilane. [b] AEAP3, *N*-(2-aminoethyl)-3-aminopropyltrimethoxysilane; AHAP3, *N*-(6-aminohexyl)aminopropyltrimethoxysilane. [c] Balance TEOS or TMOS. [d] Obtained by elemental analyses within 0.3% error. [e] Amine concentration is the concentration of diamine. [f] Determined by measuring the total NO concentration (t[NO]) released from the particles using a chemiluminescence nitric oxide analyzer. [g] Reference 33. Amine-modified silica particles were prepared via the surface-grafting method.

evidenced by pH-dependent NO release behavior (Supporting Information).

Although a diverse range of NO release properties was obtained from the silica prepared via combination of TEOS and AHAP3, AEAP3, or AEMP3, the aminoalkoxysilane content was limited to <20 mol % due to aggregation resulting from hydrogen-bonding interactions between amines and adjacent silanols and/or other amines.[47] The synthesis of particles using TMOS as the backbone precursor was thus evaluated as a strategy for increasing the aminoalkoxysilane concentration and bolstering NO storage capacity since the rate of TMOS hydrolysis is faster than that of TEOS.[36,42] Accelerated hydrolytic polycondensation reactions (i.e., quick production and consumption of silanols) would be expected to reduce potential amine−silanol and/or amine−amine interactions during particle formation. As shown in Table 1, the concentration of aminoalkoxy ligand that could be used to prepare nonaggregated particles approached 77 and 87 mol % for AHAP3- and AEAP3-based TMOS particles, respectively. Similar to TEOS, the diameter of TMOS-derived particles decreased with increasing aminoalkoxysilane concentration (from 270 to 58 nm for 10 to 87 mol % AEAP3 and from 64 to 48 nm for 10 to 70 mol % AHAP3, respectively).

Surprisingly, the NO payload of aminoalkoxysilane/TMOS particles prepared using 10 mol % aminoalkoxysilane was slightly lower than that for similarly prepared TEOS silica (145 vs 46 nmol·mg^{-1} and 380 vs 101 nmol·mg^{-1} for 10 mol % AEAP3 and AHAP3, respectively) (Table 1), indicating that the immobilization efficiency of the aminoalkoxy ligand depends on the tetraalkoxysilane backbone. Both ^{29}Si NMR (Supporting Information) and elemental analyses (Table 2) indicate that the levels of aminoalkoxy ligands in the silica particles are not directly proportional to the aminoalkoxysilane concentration in the sol. Indeed, the e_{immo} of AEAP3/TMOS silica ranged from 0.5 to 0.9, 3−5 times less than that of AEAP3/TEOS (e_{immo} = 2.1−2.6). Nevertheless, the t[NO] and [NO]$_m$ from AHAP3/TMOS silica were significantly enhanced (up to 1780 nmol·mg^{-1} and 2810 ppb·mg^{-1}, respectively) relative to those of the TEOS

(47) McKittrick, M. W.; Jones, C. W. *Chem. Mater.* **2003**, *15*, 1132−1139.

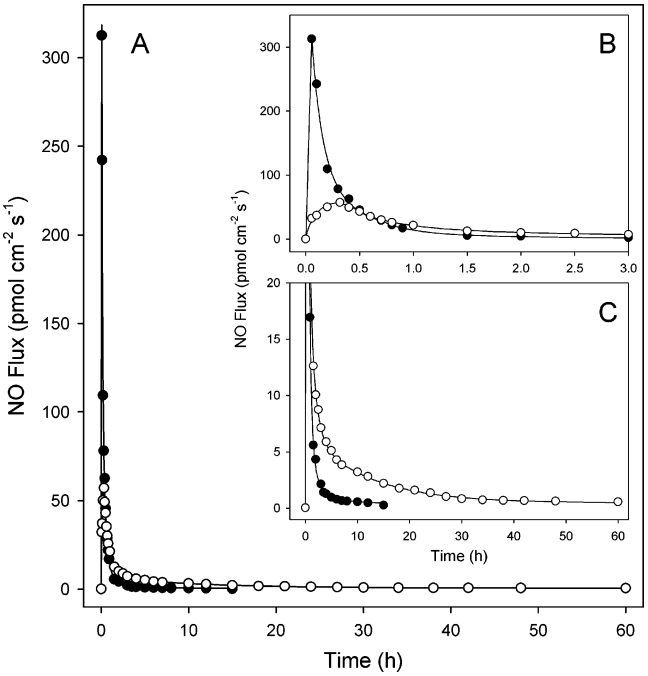

Figure 4. (A) NO release profiles of silica (*N*-diazeniumdiolate-modified 77 mol % AHAP3/TMOS)/polymer (● tecophilic PU and ○ 3140 RTV SR) hybrid films. Inset plots (B) and (C) represent the expansion of graph (A) from 0 to 3 h and reduced NO flux levels (<20 pmol·cm^{-2}·s^{-1}) at extended periods, respectively.

silica systems. Both the $t_{1/2}$ and t_m also increased with increasing aminoalkoxysilane concentration (from 0.2 to 0.9 h and 0.07 to 0.12 h for 10 to 70 mol % AHAP3, respectively).

The NO release characteristics of *N*-diazeniumdiolate-modified silica nanoparticles are significantly expanded than those of both small molecule *N*-diazeniumdiolates and the 200−300 nm NO-releasing fumed silica prepared by surface grafting. The greatest *t*[NO], 1780 nmol·mg^{-1}, was achieved with 77 mol % AHAP3/TMOS silica, a concentration roughly 3 times greater than 2N[6]−N_2O_2 surface-grafted silica (*t*[NO] = 560 nmol·mg^{-1}) prepared using the equivalent amine precursor structure (i.e., aminohexylaminopropyl ligand).[33] The greatest $t_{1/2}$ for AHAP3/TMOS silica was 0.9 h (54 min), significantly longer than the analogous small molecule DMHD/NO ($t_{1/2}$ = 3 min). Likewise, $t_{1/2}$ of AEAP3/TEOS silica was 3.4−12 h (204−720 min) (depending on the aminoalkoxysilane concentration), while $t_{1/2}$ of the surface-grafted AEAP3 silica (i.e., 2N[2]−N_2O_2) was only 2.4 h (144 min).[33]

Nitric Oxide-Releasing Silica/Polymer Hybrid Coatings. Nitric oxide-releasing polymers have recently been employed as coatings to improve the biocompatibility of blood- and tissue-contacting sensors.[48−50] In vitro and in vivo studies have revealed that polymeric NO release represents an effective strategy for reducing biofouling and improving the analytical performance of such devices.[48−50] Indeed, NO fluxes as low as 2.2 and 5 pmol·cm^{-2}·s^{-1} have been reported as sufficient for reducing platelet and bacterial adhesion, respectively.[51,52] Despite the benefits of polymeric NO release, the rather limited NO release durations hinders the utility of such coatings. Fortunately, NO release durations may be enhanced by altering the local hydrophobicity of the NO donor system. For example, Mowery et al. reported the influence of polymer hydrophobicity on water uptake and the NO release characteristics of *N*-diazeniumdiolate NO donors doped into hydrophobic PU and poly(vinyl chloride) polymers.[53]

To explore the feasibility of modulating the duration and flux of NO from *N*-diazeniumdiolate-modified nanoparticles, *N*-diazeniumdiolate-modified 77 mol % AHAP3/TMOS silica was incorporated into tecophilic polyurethane (PU) and 3140 RTV silicone rubber (SR). Tecophilic PU, an aliphatic, polyether-based urethane block copolymer, is a medical-grade hydrogel capable of absorbing large amounts of water (up to 150 wt % of its dry resin).[54] In contrast, 3140 RTV SR is a more hydrophobic polymer used to fabricate several implantable medical devices[55] including intravascular ion and gas sensors.[56,57] As expected, the kinetics and duration of NO release from the silica particle-doped polymers varied as a function of the polymer's hydrophobicity, and thus the water uptake. The NO release (Figure 4) from silica nanoparticles dispersed in SR (water contact angle of 99.1 ± 2.5°) was characterized by a lower maximum flux and significantly lengthened NO release duration compared to those of PU (water contact angle of 66.5 ± 1.7°). Indeed, the more hydrophobic SR polymer resulted in a NO flux >2.2 pmol·cm^{-2}·s^{-1} for 20 h. Such NO flux was only maintained for 3 h from the PU polymer. This result is expected since water must first be absorbed by the polymer to initiate *N*-diazeniumdiolate decomposition and subsequent NO release.[13]

Conclusions

The synthesis of NO-releasing nanoparticles represents an important step toward the development of NO storage/delivery systems that bridge the gap between small molecule *N*-diazeniumdiolates and *N*-diazeniumdiolate-modified macromolecules. Control over both the structure and concentration of tetraalkoxy- and aminoalkoxysilane precursors allows for the preparation of NO donor-modified silica nanoparticles of widely varying sizes (*d* = 20−500 nm) and NO release properties (e.g., NO payload of 50−1780 nmol·mg^{-1}, maximum NO concentrations (10−5500 ppb·mg^{-1}), half-lives (0.1−12 h), and NO release durations (15−30 h). Silica nanoparticles prepared via a one-pot approach exhibit an increased NO payload of up to 3 times greater than that attainable via surface-grafted silica.[33] The silica nanoparticles can be embedded (i.e., doped) into polymers and their NO flux rate and duration further altered as a function of polymer hydrophobicity. Furthermore, the diversity of NO release kinetics and scaffold size and favorable toxicity represent distinct advantages for silica over previously reported nanoparticle systems. Indeed, the ability to tune both the NO storage/release characteristics and size of the silica nanoparticles may facilitate the development of new pharmaceuticals for

(48) Frost, M. C.; Meyerhoff, M. E. *Anal. Chem.* **2006**, *78*, 7370−7377.
(49) Frost, M. C.; Reynolds, M. M.; Meyerhoff, M. E. *Biomaterials* **2005**, *26*, 1685−1693.
(50) Shin, J. H.; Schoenfisch, M. H. *Analyst* **2006**, *131*, 609−615.
(51) Nablo, B. J.; Schoenfisch, M. H. *Biomacromolecules* **2004**, *5*, 2034−2041.
(52) Robbins, M. E.; Hopper, E. D.; Schoenfisch, M. H. *Langmuir* **2004**, *20*, 10296−10302.
(53) Mowery, K.; Schoenfisch, M. H.; Baliga, N.; Wahr, J. A.; Meyerhoff, M. E. *Electroanalysis* **1999**, *11*, 681−686.
(54) Technical information obtained from Noveon, Inc. (http://www.estane.com/),January 2007.
(55) Donaldson, P. E. K.; Sayer, E. *Med. Biol. Eng. Comput.* **2006**, *15*, 712−715.
(56) Frost, M. C.; Rudich, S. M.; Zhang, H.; Maraschio, M. A.; Meyerhoff, M. E. *Anal. Chem.* **2002**, *74*, 5942−5947.
(57) Shin, J. H.; Sakong, D. S.; Nam, H.; Cha, G. S. *Anal. Chem.* **1996**, *68*, 221−225.

medical conditions and/or diseases requiring NO-based therapy. Recent work suggests that the size of the delivery vehicle is particularly important in determining cellular/tissue uptake and accumulation, with particles having a diameter between 20 and 100 nm being most optimal.[58−60] The NO-releasing silica nanoparticles synthesized herein fit this range. The silica particles also avoid some practical limitations of previously reported nanoconstructs (e.g., dendrimers) in that their synthesis and purification are simple and their precursors inexpensive. Since concentration dictates NO's biological action, a scaffold with wide-ranging NO payloads and NO release kinetics may prove useful for a range of applications (e.g., picomolar to nanomolar for regulating vasodilation and angiogenesis and submicromolar to micromolar for killing bacteria or tumor cells).

(58) Kumar, C. S. S. R.; Hormes, J.; Leuschner, C. *Nanofabrication Towards Biomedical Applications: Techniques, Tools, Applications, and Impact*; Wiley-VCH: Weinheim, Germany, 2005.
(59) Chithrani, B. D.; Ghazani, A. A.; Chen, W. C. W. *Nano Lett.* **2006**, *6*, 662−668.
(60) Schwartzberg, A. M.; Olson, T. Y.; Talley, C. E.; Zhang, J. Z. *J. Phys. Chem. B* **2006**, *110*, 19935−19944.

Acknowledgment. The authors thank Professor Paul Edmiston of the College of Wooster for surface area/pore size analysis and Marc ter Horst of the NMR Analysis Laboratory at the University of North Carolina at Chapel Hill for helpful discussion and technical assistance. This research was supported by the National Institutes of Health (NIH EB000708).

Supporting Information Available: Schematics of the sol−gel process, chemical structures of the aminoalkoxysilanes used in this study, solid-state ^{29}Si NMR data for functionalized silica particles, and effect of pH on NO release. This material is available free of charge via the Internet at http://pubs.acs.org.

JA0674338